Journal of
BIOPHOTONICS
4/13
www.biophotonics-journal.org

Reflectance Confocal Microscopy (RCM)

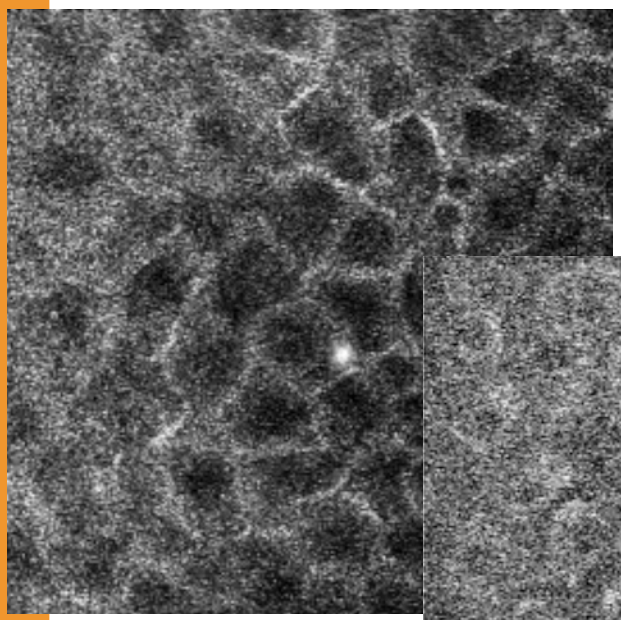

Multiphoton Microscopy (MPM)

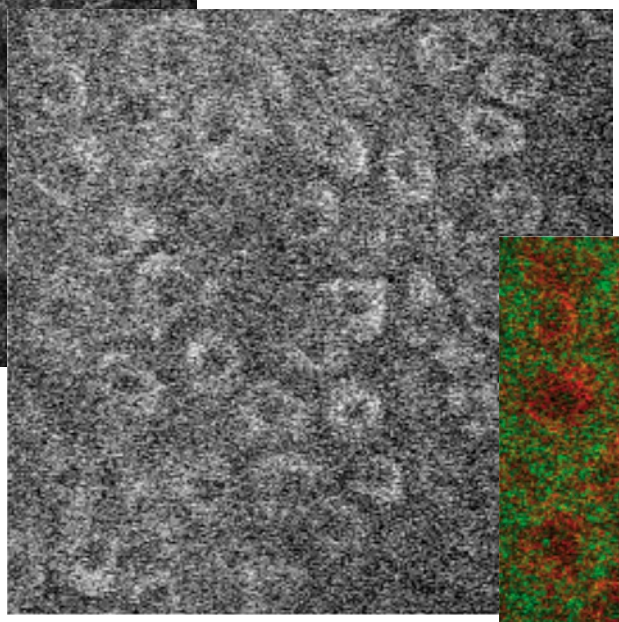

False Color Overlay
Green = RCM
Red = MPM

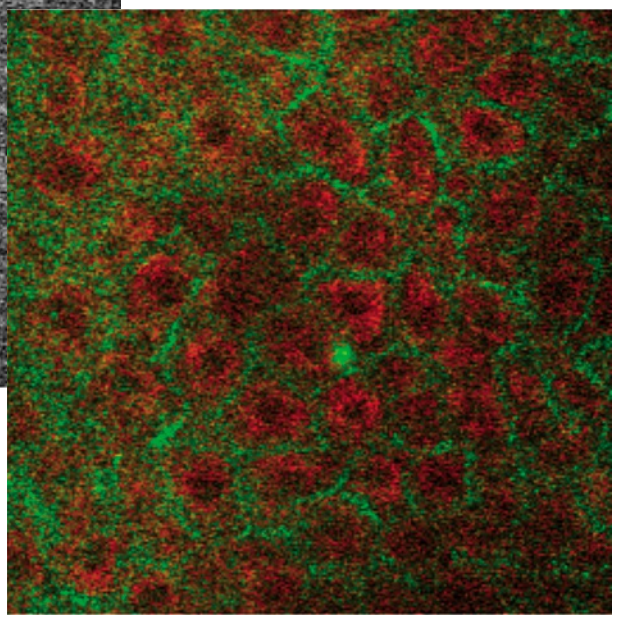

***In vivo* video-rate, co-registered multiphoton and reflectance confocal imaging of skin**
H. Wang, A. M. D. Lee, Z. Frehlick, H. Lui, D. I. McLean, S. Tang, and H. Zeng

WILEY-VCH
ISSN 1864-063X J. Biophotonics, Vol. **6**, No. 4 (April), 299–382 (2013)
Impact Factor 2011: 4.343

Journal of
www. biophotonics-journal.org
BIOPHOTONICS

WILEY-VCH

J. Biophotonics **6**, No. 4, 305–309 (2013) / **DOI** 10.1002/jbio.201200067

Journal of BIOPHOTONICS

LETTER

Perfectly registered multiphoton and reflectance confocal video rate imaging of *in vivo* human skin

Hequn Wang[**,1], *Anthony M.D. Lee*[**,1,2], *Zack Frehlick*[1], *Harvey Lui*[1,3], *David I. McLean*[1,3], *Shuo Tang*[4], *and Haishan Zeng*[*,1,2,3]

[1] Imaging Unit – Integrative Oncology Department, British Columbia Cancer Agency Research Centre, Vancouver, BC, Canada
[2] Department of Physics and Astronomy, University of British Columbia, Vancouver, BC, Canada
[3] Photomedicine Institute, Department of Dermatology and Skin Science, University of British Columbia and Vancouver Coastal Health Research Institute, Vancouver, BC, Canada
[4] Department of Electrical and Computer Engineering, University of British Columbia, Vancouver, BC, Canada

Received 13 April 2012, revised 1 June 2012, accepted 17 June 2012
Published online 3 July 2012

Key words: multiphoton microscopy, reflectance confocal microscopy, *in vivo* video microscopy, skin diagnosis

Supporting information for this article is available free of charge under http://dx.doi.org/10.1002/jbio.201200067

We present a multimodal *in vivo* skin imaging instrument that is capable of simultaneously acquiring multiphoton and reflectance confocal images at up to 27 frames per second with 256×256 pixel resolution without the use of exogenous contrast agents. A single femtosecond laser excitation source is used for all channels ensuring perfect image registration between the two-photon fluorescence (TPF), second harmonic generation (SHG), and reflectance confocal microscopy (RCM) images. Images and videos acquired with the system show that the three imaging channels provide complementary information in *in vivo* human skin measurements. In the epidermis, cell boundaries are clearly seen in the RCM channel, while cytoplasm is better seen in the TPF imaging channel, whereas in the dermis, SHG and TPF channels show collagen bundles and elastin fibers, respectively. The demonstrated fast imaging speed and multimodal imaging capabilities of this MPM/RCM instrument are essential features for future clinical application of this technique.

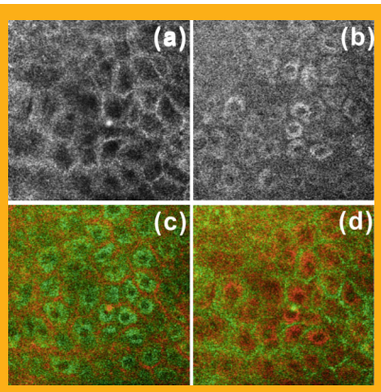

(**a**) RCM, (**b**) SHG + TPF, (**c**) false color overlay of SHG + TPF (green) and RCM (red), and (**d**) false color overlay of SHG + TPF (red) and RCM (green) images from the dorsal forearm of a 41-year-old Asian male volunteer. Excitation wavelength $\lambda = 720$ nm. FOV $= 150 \times 150$ μm. Resolution $= 256 \times 256$ pixels. Frame rate $= 15$ fps.

* Corresponding author: e-mail: hzeng@bccrc.ca, Phone: +1 604 675 8083, Fax: +1 604 675 8099
** These authors contributed equally to this work.

Journal of
BIOPHOTONICS

1. Introduction

The development of non-invasive diagnostic imaging techniques for examining the microstructure of skin is important because the standard examination practice of biopsy leads to scarring. Two techniques that have garnered much interest in recent years for dermatology use are reflectance confocal microscopy (RCM) and multiphoton microscopy (MPM). The optical sectioning capability of RCM has allowed *in vivo*, high resolution morphological images of skin [1]. MPM also has inherent optical sectioning capability due to the nonlinear excitation process that obviates the need for a pinhole to reject out-of-focus light. Different MPM excitation mechanisms are sensitive to different biochemical components of tissue. For example, two-photon fluorescence (TPF) signals arise from endogenous fluorophores of skin components such as elastin, NAD(P)H, and keratin; while second harmonic generation (SHG) is sensitive to non-centrosymmetric structures such as collagen [2–3]. As there is less scattering and absorption of the near infrared lasers used in MPM, there is deeper penetration as well as less photo-damage to the tissue compared to the equivalent single photon excitation laser [3–4].

Combining both RCM and MPM imaging (hereby called RCM/MPM imaging) potentially allows greater clinical diagnostic utility as complementary information can be revealed using the two techniques. Indeed there have been a number of studies of this nature involving both *ex vivo* and *in vivo* tissue imaging. Images of *ex vivo* porcine skin and bovine cornea using RCM/MPM imaging have shown that cell nuclei can be detected in the reflectance confocal signal, while the multiphoton autofluorescence signal can be used for cytoplasmic imaging through the entire epithelium [5]. Similarly, *ex vivo* human skin studies have demonstrated that cell borders are more clearly seen from the reflected confocal signal, while the autofluorescence signal provides cytoplasmic details [6, 7]. *In vivo* RCM and MPM imaging have also been used together to evaluate skin diseases such as seborrheic keratosies, angiomas, and actinic keratoses, but without co-registration of the two imaging modes [8].

For clinical application, *in vivo* imaging is preferred over *ex vivo* imaging because it does not necessitate tissue removal. It also leaves the tissue in its native state, whereas *ex vivo* tissue can be subject to biochemical/structural changes due to the degradation of the sample, tissue contraction, and elimination of living tissue dynamics such as blood perfusion and oxygenation.

With respect to *in vivo* skin imaging, the previously reported studies that have measured RCM and MPM have serious limitations. This type of imaging is difficult because patient motion must be mitigated, and often multiple lesion sites or large lesions must be examined. Various motion compensation approaches such as real-time adaptive focus control [9] have been applied for reducing motion artifacts, suitable for imaging fast dynamics in a single focal plane. Surveying a tissue volume by imaging through many focal planes, while also limiting motion artefact can be simultaneously handled by imaging with as high frame rate as possible. Video rate imaging has been demonstrated in RCM [10] and MPM [11] alone, but not in a combined RCM/MPM system.

Another important issue with *in vivo* RCM/MPM imaging is ensuring image registration between the RCM and MPM channels. If entirely different optical systems are used to measure the RCM and MPM channels separately, image registration is not guaranteed [8, 12]. Systems have been developed that use the same objective for both imaging modalities by multipassing the tissue with two laser sources, however RCM/MPM image registration is still not ensured as the patient can still move between passes [13–15]. Another system has scanned RCM and MPM with the same objective simultaneously with different wavelengths but image registration can still be problematic as two different scanning mechanisms were used [16]. The problem of image registration can be solved definitively if a single laser source is used and is scanned with the same mechanism while imaging with both the RCM and MPM channels. This type of system has been developed but has only been demonstrated using *ex vivo* specimens [5, 7]. Here we adapt this latter approach to present a RCM/MPM system that captures perfectly registered RCM and MPM (both SHG and TPF) images at up to 27 frames per second (fps). We use this system to capture *in vivo* skin images.

2. Experimental

Our system setup is shown schematically in Figure 1. As it is based on our MPM system that has been published previously, we omitted some details of the system, which can be found elsewhere [11]. Briefly, the output from a tunable (720–950 nm) femtosecond Ti:Sa excitation laser was scanned over the back aperture of a 60X (NA = 1.0) water-immersion objective using an 8 kHz resonance scanner for the fast axis and a galvanometer scanner for the slow axis. The maximum field of view (FOV) for the system was 300×300 μm. Acquiring images with 256 or 512 lines generated frame rates of 27 fps or 15 fps respectively. The MPM channels were collected in the epi-direction using a 665 nm longpass dichroic beamsplitter. Two modes were used to collect the MPM signals: one where both the TPF and the SHG signals were integrated into a single PMT (SHG + TPF mode); and the other where insertion of another dichroic beamsplitter, filters and use of two PMTs allowed se-

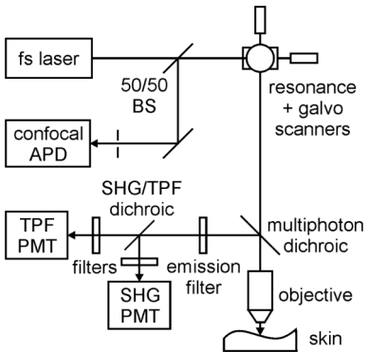

Figure 1 *In vivo* video rate RCM/MPM system setup. The SHG/TPF dichroic and filters preceding PMTs were changed or removed according to the desired imaging modalities. Lenses have been omitted from the diagram for clarity.

paration of the TPF and SHG images. A 50/50 beamsplitter was used to direct the descanned RCM signal to a lens ($f = 150$ mm) that focused the light through a 50 μm pinhole to an avalanche photodiode (APD) module (C10508, Hamamatsu Corp., Bridgewater, NJ). The RCM, TPF, and SHG images were recorded by a 10-bit multichannel frame grabber (Helios eA, Matrox Electronic Systems Ltd., Dorval, QC, Canada) as synchronized independent video streams. As the resonance scanner operates bidirectionally, the forward and backward passes of each line were added in real-time. Real-time correction of the resonance scanner sinusoidal image distortion was also applied. The pixel clock was matched to the PMT amplifier bandwidth and pixels were re-binned to reduce the frame size to 256×256 pixels. As all the imaging channels share the same laser, scanners, and objective, the RCM, TPF, and SHG images are perfectly registered, ensuring with complete certainty that the images are comparable.

To reduce involuntary subject motion a metal ring was affixed to the imaging location with double-sided tape. The ring mated magnetically to the objective frame via a manually driven micrometer-actuated 3-axis translation stage that controlled the imaging location and focal plane depth. Only water was present between the objective and the skin surface. The laser power incident on the skin at all wavelengths was adjusted to be 40 mW using a half-waveplate/polarizer combination at the laser exit. The study was approved by the University of British Columbia Research Ethics Board (#H96-70499). Informed consent was obtained from each volunteer subject.

3. Results and discussion

Figures 2 and 3 show the RCM, SHG + TPF, and their false color overlay skin images using 720 nm

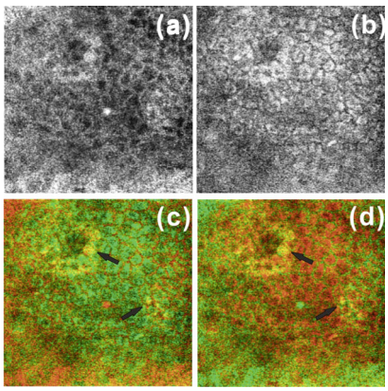

Figure 2 (**a**) RCM, (**b**) SHG + TPF, (**c**) false color overlay of SHG + TPF (green) and RCM (red), and (**d**) false color overlay of SHG + TPF (red) and RCM (green) images from the stratum basale (SB) of the dorsal forearm of a Caucasian male in his early 50s. Excitation wavelength $\lambda = 720$ nm. FOV $= 170 \times 170$ μm. Resolution $= 256 \times 256$ pixels. Frame rate $= 15$ fps.

excitation. As previously reported [10], shorter wavelengths provide better MPM imaging contrast in epidermis. At shorter excitation wavelengths where tissue penetration is shallow and the MPM signals are only TPF, it is better to image with a single PMT because the detection path length can be made shorter to increase the signal collection efficiency.

The RCM (Figure 2a) and SHG + TPF (Figure 2b) images near the stratum basale (SB) layer of a Caucasian male in his early 50's are shown overlaid in false color in Figure 2c and d with different color coding. Images in Figure 2 were extracted from Video 1 (Supplementary material), which is a 15 fps *in vivo* false color overlay (RCM = red, SHG + TPF = green) movie increasing in depth from near the skin surface to near the dermal/epidermal junction (DEJ). Based on the anatomical features seen in the images and video, the imaging depth extends from the skin surface to approximately 150 μm below the surface. Precise imaging depths are not recorded in this work because subject motion occurs on a faster timescale than our ability to read the micrometers. However, the fast frame rate of our system appears to mitigate subject motion such as blurring and smearing artefact in individual video frames. The images and video clearly show the complementary nature of the RCM and MPM imaging modalities. The honey-comb shaped cells in the stratum spinosum (SS) show bright cell boundaries in the RCM channel while bright cytoplasm is seen in the SHG + TPF channel. Deeper at the DEJ, dermal papilla and cellular structures are well visualized in both the RCM and SHG + TPF channels. Some basal cells at the DEJ are bright in both the RCM and SHG + TPF imaging channels (yellow in false color overlay,

Journal of
BIOPHOTONICS

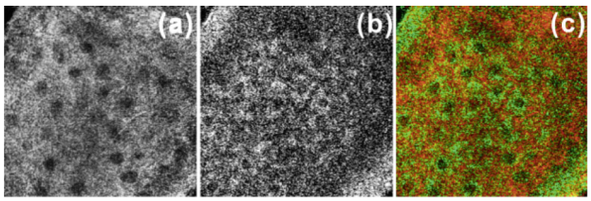

Figure 3 (**a**) RCM, (**b**) SHG + TPF, and (**c**) false color overlay of SHG + TPF (green) and RCM (red) images from the stratum granulosum (SG) of the dorsal forearm of a 41-year-old Asian male. Excitation wavelength $\lambda = 720$ nm. FOV $= 150 \times 150$ µm. Resolution $= 256 \times 256$ pixels. Frame rate $= 27$ fps.

noted by arrows in Figures 2c, 2d). We believe these cells contain melanin, which is both highly scattering and fluorescent [17, 18]. The bright dot near the center of all of the RCM images and videos is an artifact due to reflection from one of the lenses in the optical system.

Figure 3 shows the RCM (Figure 3a), SHG + TPF (Figure 3b), and false color overlay images (Figure 3c) from the stratum granulosum (SG) layer of a 41-year-old Asian male. Images in Figure 3 were extracted from Video 2, which is a 27 fps false color overlay (RCM = red, SHG + TPF = green) *in vivo* movie increasing in depth from near the skin surface to near the stratum basale (SB). As expected, the almost doubling of the frame rate in Video 2 (Figure 3) compared to Video 1 (Figure 2) results in reduced image quality as less pixel averaging leads to a lower signal to noise ratio.

Figure 4 shows RCM/MPM imaging from the inner forearm of a 64-year-old Caucasian male under 880 nm excitation. Using this longer wavelength permits deeper imaging into the skin dermis. Images from the reticular dermis (RD) are shown in the figure. For these images, a 458 nm dichroic beamsplitter, and 440/40 nm bandpass and 458 nm longpass filters were used in the detection arm to separate the MPM signals onto SHG and TPF PMTs respectively. The simultaneously acquired RCM (Figure 4a), TPF (Figure 4b), and SHG (Figure 4c) can be viewed separately or overlaid in false color (Figure 4d). These images were extracted from Video 3, a 15 fps false color overlay (RCM = red, TPF = green, SHG = blue) *in vivo* video varying in depth through the RD.

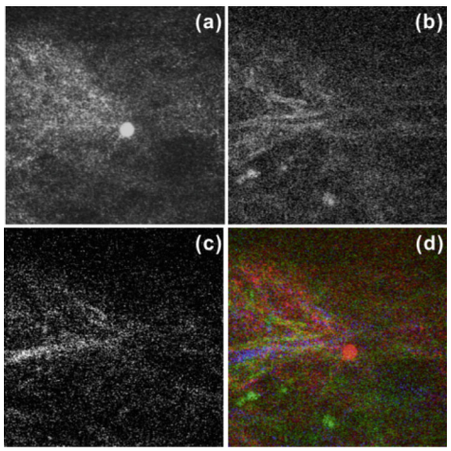

Figure 4 (**a**) RCM, (**b**) TPF, (**c**) SHG, and (**d**) false color overlay of RCM (red), TPF (green), and SHG (blue) images from the reticular dermis (RD) of the inner forearm of a 64-year-old Caucasian male. Excitation wavelength $\lambda = 880$ nm. FOV $= 150 \times 150$ µm. Resolution $= 256 \times 256$ pixels. Frame rate $= 15$ fps.

The RCM image shows rather diffuse fiber structures, while the TPF and SHG channel fiber structures appear finer and more pronounced. The fibers in the SHG channel are collagen while those in the TPF channel are elastin. Also present in the TPF channel (green in Video 3) are globular structures that we speculate to be granular elastic tissues which are usually present in sun-damaged skin.

Other researchers have had success in reducing subject motion using a coverslip between the objective and the skin allowing image averaging over several seconds. Using a coverslip should also allow us to improve our imaging stability and allow multiple frame averaging for improving image quality. However, it is ultimately desirable to have imaging rates as fast as possible. As RCM and MPM are depth resolved techniques, to perform volumetric imaging, fast frame rates, such as the video frame rate we demonstrate here, are essential. It is envisioned that further development of RCM/MPM imaging will lead to instruments that can provide diagnostic information comparable to histopathology without the need for excising tissue.

4. Conclusion

In summary, we demonstrate an RCM/MPM instrument capable of simultaneously imaging human skin *in vivo* at up to 27 fps. By using the same laser source for RCM, SHG, and TPF imaging channels, we ensure that they are perfectly registered. These unique RCM/MPM system features are essential advances that are necessary for future clinical applications of RCM/MPM.

Acknowledgements This work was supported by the Canadian Dermatology Foundation, the VGH & UBC Hospital Foundation, the BC Hydro Employees Community Services Fund, and the BC Cancer Agency. AMDL acknowledges MSFHR and CIHR-SRTC for postdoctoral funding. HW acknowledges CIHR-SRTC for doctoral funding.

References

[1] P. Calzavara-Pinton, C. Longo, M. Venturini, R. Sala, and G. Pellacani, Photochem. Photobiol. **84**, 1421 (2008).
[2] W. R. Zipfel, R. M. Williams, R. Christie, A. Y. Nikitin, B. T. Hyman, and W. Webb, Proc. Natl. Acad. Sci. U.S.A. **100**, 7075 (2003).
[3] T. Tsai, S. Jee, C. Dong, and S. Lin, J. Dermatol. Sci. **56**, 1 (2009).
[4] K. Konig, J. Biophotonics **1**, 13 (2008).
[5] W. Chen, C. Chou, M. Lin, Y. Chen, S. Jee, H. Tan, T. Tsai, K. Kim, D. Kim, P. T. C. So, and S. Lin, J. Biomed. Opt. **14**, 054026 (2009).
[6] M. Lin, W. Chen, W. Lo, H. Tan, T. Tsai, S. Jee, S. Lin, and C. Dong, Proc. SPIE **6424**, 64240E (2007).
[7] S. H. Choi, W. H. Kim, Y. J. Lee, H. Lee, W. J. Lee, J. D. Yang, J. W. Shim, and J. Kim, J. Opt. Soc. Korea **15**, 61 (2011).
[8] M. J. Koehler, M. Speicher, S. Lange-Asschenfeldt, E. Stockfleth, S. Metz, P. Elsner, M. Kaatz, and K. Konig, Exp. Dermatol. **20**, 589 (2011).
[9] S. Laffray, S. Pages, H. Dufour, P. De Koninck, Y. De Koninck, and D. Cote, PLoS ONE **6**, e19928 (2011).
[10] M. Rajadhyaksha, R. R. Anderson, and R. H. Webb, Appl. Opt. **38**, 2105 (1999).
[11] A. M. D. Lee, H. Wang, Y. Yu, S. Tang, J. Zhao, H. Lui, D. I. McLean, and H. Zeng, Opt. Lett. **36**, 2865 (2011).
[12] B. R. Masters and P. T. C. So, Opt. Express **8**, 2 (2001).
[13] W. Chen, Y. Sun, W. Lo, H. Tan, and C. Dong, Microsc. Res. Techniq. **71**, 83 (2008).
[14] S. M. Zhuo, J. X. Chen, X. S. Jiang, K. C. Lu, and S. S. Xie, Laser Phys. Lett. **5**, 614 (2008).
[15] W. Chen, W. Lo, Y. Sun, S. Lin, H. Tan, and C. Dong, Proc. SPIE **6138**, 61380M (2006).
[16] R. Hendriks and G. Lucassen, Proc. SPIE **4262**, 287 (2001).
[17] M. Rajadhyaksha, M. Grossman, D. Esterowitz, R. H. Webb, and R. R. Anderson, J. Invest. Dermatol. **104**, 946 (1995).
[18] L. H. Laiho, S. Pelet, T. M. Hancewicz, P. D. Kaplan, and P. T. So, J. Biomed. Opt. **10**, 024016 (2005).